

Electronic Supplementary Information

**One-step implementation of plasmon enhancement and solvent
annealing effects for air-processed high-efficiency perovskite solar
cells†**

Yan Guo,^a Xiong He,^a Xin Liu,^b Xin Li^{*ab} and Leilei Kang^{*c}

^a MIIT Key Laboratory of Critical Materials Technology for New Energy Conversion and Storage, School of Chemistry and Chemical Engineering, Harbin Institute of Technology, Harbin 150001, China.

^b State Key Lab of Urban Water Resource and Environment, Harbin Institute of Technology, Harbin 150090, China.

^c Dalian Institute of Chemical Physics, Chinese Academy of Sciences, Dalian 116023, China.

*Address correspondence to: lixin@hit.edu.cn (X. Li); leikang@dicp.ac.cn (L.L. Kang)

Experimental section

2.1 Materials

Cetyl trimethyl ammonium bromide ($C_{19}H_{42}BrN$, CTAB, > 99 %) was purchased from Sigma-Aldrich. Sodium borohydride ($NaBH_4$, 98 %), L-ascorbic acid, hydrogen tetrachloroaurate(III) trihydrate ($HAuCl_4 \cdot 3H_2O$, 99 %), zinc acetate dihydrate ($Zn(CH_3COO)_2 \cdot 2H_2O$, 99.995 %) were obtained from Aladdin. Lead iodide (PbI_2 , 99.999 %) and 4-tert-butylpyridine and lithium bis(trifluoromethanesulfonyl)imide (Li-TFSI, 99.9 %) were acquired from Kanto. Silver nitrate ($AgNO_3$, 99.8 %), potassium hydroxide (KOH, 95 %), methylammonium iodide (CH_3NH_3I , > 99 %) and 2, 2', 7, 7'-tetrakis-(N, N-di-4-methoxyphenylamino)-9, 9' spirobifluorene (Spiro-OMeTAD, 99.85 %) were respectively purchased from Energy Chemical, Tianjin Fengchuan Chemical Reagent Technologies Co., Ltd, Youxuan Trade and Toronto Technologies Co., Ltd. Other anhydrous solvent were purchased from J&K Chemical. Where all reagents were used as received without any further purification.

2.2 Preparation of ZnO nanoparticles

The ZnO nanoparticles (NPs) were synthesized following a procedure described in our previous work.¹ In a typical procedure, 2.36 g $Zn(CH_3COO)_2 \cdot 2H_2O$ was first dissolved in 100 mL of methanol solution. Then, 52 mL of KOH methanol solution (354 mM) was added dropwise into the aforementioned solution. Subsequently, the mixture was kept at 65 °C for 2.5 h under magnetic stirring, leading to the production of ZnO NPs. Then, the obtained ZnO NPs were washed with anhydrous methanol for three times to remove residual precursors. Finally, the ZnO NPs were dispersed into a solution of n-butanol-chloroform-methanol (14:1:1 volume ratio) to form a 20 mg/mL ZnO NPs suspension.

2.3 Preparation of Au nanorods

Au nanorods (NRs) were synthesized by a seed-mediated growth method, according to a reported procedure with some modification.² Firstly, 0.6 mL of 10 mM NaBH₄ aqueous solution was added to 10 mL of 100 mM CTAB aqueous solution containing 0.25 mM HAuCl₄ under stirring conditions. The mixed solution was vigorously stirred for 10 min before being transferred to a 30 °C water bath where it was left to stay for 12 hours resulting in a formation of brownish yellow Au seeds solution. In order to synthesize the Au NRs, 1 mL of 10 mM AgNO₃, 5 mL of 10 mM HAuCl₄, 1.6/0.8/0.4/0.2 mL of 2 M HCl, 0.55 mL of 100 mM ascorbic acid and 0.12 mL of Au seeds solution were sequentially added to 95 mL of 100 mM CTAB aqueous solution, and undisturbedly reacted overnight under room temperature. The resulting products were collected by centrifugation, and then the NRs were washed with deionized water for one time. Finally, the equivalent volume of Au NRs with different aspect ratio was redispersed in N, N-dimethylformamide (DMF), forming a 0.5 M suspension.

2.4 Fabrication of ZnO-based PSCs

All ZnO-based PSC devices were fabricated on FTO glass substrates (1.5 cm × 2.0 cm). FTO substrates were first etched by zinc powder and 6 M HCl, and ultrasonically cleaned successively with detergent, deionized water, acetone, 2-propanol, ethanol, followed by an UV-ozone treatment for 20 min. After that, the electron transport material was deposited onto the substrates by spin-coating ZnO solution at 500 rpm. for 3 s and 3000 rpm. for 30 s and dried at room temperature for 10 min. This process was repeated two times to obtain a compact ZnO film. Then, the ZnO film was aged 24 h under ambient conditions. Subsequently, the Au NRs DMF suspension (0.5 M) was spin-coated onto the surface of FTO/ZnO at 500 rpm. for 5 s and 1500 rpm. for 60 s and then dried at 30 °C for 10 min. The perovskite layer was synthesized by a two-step

spin-coating fabrication protocol. The PbI_2 DMF solution (460 mg /mL) was first spin-coated on the FTO/ZnO film at 3000 rpm. for 30 s and annealed at 70 °C for 10 min. Then, a solution of $\text{CH}_3\text{NH}_3\text{I}$ in 2-propanol (50 mg/mL) was spin-coated on the surface of PbI_2 film at 1000 rpm. for 5 s and 3000 rpm. for 25 s and annealed at 80 °C for 30 min in a closed petri dish to form a highly crystalline and compact without pinhole $\text{CH}_3\text{NH}_3\text{PbI}_3$ (MAPbI₃) layer. After the FTO/ZnO/Au NRs/MAPbI₃ films were cooled down to the room temperature, the Spiro-OMeTAD hole transfer layer (80 mg of Spiro-OMeTAD, 28.5 μL 4-tert-butylpyridine, 17.5 μL Li-TFSI (520 mg of Li-TFSI in 1 mL of acetonitrile) all dissolved in 1 mL chlorobenzene) was deposited on the top of FTO/ZnO/MAPbI₃ film by spin-coating at 4000 rpm. for 30 s. Finally, about 60 nm thick Au counter electrode was deposited on top of Spiro-OMeTAD film via vacuum thermal evaporation at an evaporation rate 1.0 Å/s. As a control experiment, the PSC devices without Au NRs were fabricated under the same fabrication conditions as well. In order to further investigate the possible improvement mechanisms of perovskite crystal, we also designed and fabricated the films of ZnO/MAPbI₃, ZnO/Au NRs/MAPbI₃ and ZnO/DMF/MAPbI₃ films according to the above operating procedure. The active area of PSCs was confirmed to be 0.12 cm² by a non-reflective metal mask. All processes including fabrication, measurement and storage of devices were carried out under ambient conditions. The environmental temperature and relative humidity for the fabrication process, *J-V* measurement and photo-stability investigation were about 25 °C and 50 %, respectively. The average relative humidity was about 40 % when studying the long-term ambient atmosphere stability.

2.5 Characterization

X-ray absorption near edge structure (XANES) at the Zn K-edge (9659 eV) were recorded at the BL14W1, Shanghai Synchrotron Radiation Facility (SSRF), Shanghai

Institute of Applied Physics (SINAP), China. The energy was calibrated by Zn foil. The spectra were collected at room temperature via the fluorescence mode. The light source is portable xenon lamp. X-ray diffraction (XRD) pattern was used to analyze crystal structure, which was recorded on a Panalytical Empyrean X-ray diffractometer with a Cu K α radiation ($\lambda = 1.540598 \text{ \AA}$) at a scan rate of $2^\circ/\text{min}$. The morphologies of nanoparticles and films as well as the element EDS mappings were analyzed by Cold Field Emission scanning electron microscopy (SEM, Hitachi, SU8000) and transmission electron microscope (TEM, JEOL, JEM-2100). Atomic force scanning probe microscope (AFM, Bruker, Dimension Icon) was used to perform AFM high image and scanning Kelvin probe microscope (SKPM) tests. Photoluminescence (PL) spectra and PL mappings were performed on a Renishaw in Via confocal micro-Raman spectroscopy system ($\lambda = 633$ or 532 nm). Ultraviolet-visible (UV-vis) absorption spectroscopy measurements were conducted on TU1901 spectrometer (Beijing Purkinje General Instrument Co., Ltd). Static water contact angle was tested using a JC2000C1 contact angle instrument.

Photocurrent density-photovoltage (J - V) curves of PSCs and conductivity tests were measured by a binding unit of electrochemical workstation (VersaSTAT 3, Ametek, USA) and a class ABB solar simulator (model 94021A, Newport, USA), where the cells were illuminated using an AM 1.5G sunlight (100 mW cm^{-2}) generating from 150 W xenon lamp optical source, and the intensity of light was standardized by a Newport Oriel standard PV reference cell system (model 91150 V). The scan rate was 0.2 V/s . Electrochemical impedance spectra (EIS) were performed using a VersaSTAT 3 electrochemical workstation (Ametek, USA) at a frequency ranging from 10^6 to 0.1 Hz with 5 mV amplitude in the dark condition. The EIS data was fitted by the software of ZView2 according to the equivalent circuit model. Incident photon-to-electron

conversion efficiency (IPCE) was recorded by a QTest Station 500D solar cell quantum efficiency measurement system (CROWNTECH, USA) equipped with a 300 W tungsten lamp power source, a QEM11-S 1/8 m monochromator, a Keithley 2000 multimeter and an opaque chamber. Hall data were collected by a Hall 8800 system.

Table S1 Summary of references about application of Au or Ag NPs in PSCs.

Device structure	Preparations conditions	J_{sc} (mA cm ⁻²)	V_{oc} (V)	FF (%)	PCE (%)	Ref.
FTO/ZnO/Au NRs/CH ₃ NH ₃ PbI ₃ /Spiro-OMeTAD/Au		22.52	-1.026	71.45	16.51	Current
FTO/ZnO/CH ₃ NH ₃ PbI ₃ /Spiro-OMeTAD/Au	In Air	20.58	-1.021	68.86	14.47	Work
FTO/c-TiO ₂ /Au@SiO ₂ -m-Al ₂ O ₃ /MAPbI _{3-x} Cl _x /Spiro-OMeTAD/Ag		16.91	-1.02	64	11.4	Ref. 12
FTO/c-TiO ₂ /m-Al ₂ O ₃ /MAPbI _{3-x} Cl _x /Spiro-OMeTAD/Ag	In air	14.76	-1.04	67	10.7	
FTO/c-TiO ₂ /m-TiO ₂ @Au NSs/Triple cation perovskite/Spiro-OMeTAD/Au	N ₂ -filled	22.97	-1.08	71	17.72	Ref. 13
FTO/c-TiO ₂ /m-TiO ₂ /Triple cation perovskite/Spiro-OMeTAD/Au	glove box	21.14	-1.05	69	15.19	
FTO/c-TiO ₂ /m-TiO ₂ -Au@Ag nanocuboids/CH ₃ NH ₃ PbI _{3-x} Cl _x /Spiro-OMeTAD/Au	Glovebox	23.6	-1.04	74.6	18.31	Ref. 14
FTO/c-TiO ₂ /m-TiO ₂ /CH ₃ NH ₃ PbI _{3-x} Cl _x /Spiro-OMeTAD/Au		21.13	-1.01	74.1	15.56	
FTO/ZnO/CH ₃ NH ₃ PbI ₃ /mPEG-Au NSs@Spiro-OMeTAD/Ag	N ₂ -filled	18.65	-1.053	72.59	13.97	Ref. 15
FTO/ZnO/CH ₃ NH ₃ PbI ₃ /Spiro-OMeTAD/Ag	glove box	17.78	-1.034	69.66	12.49	
FTO/c-TiO ₂ /p-TiO ₂ -Au@TiO ₂ NRs/CH ₃ NH ₃ PbI ₃ -Au@TiO ₂ NRs/Spiro-OMeTAD/Ag	A	23.12	-1.04	75.5	18.24	Ref. 16
FTO/c-TiO ₂ /p-TiO ₂ /CH ₃ NH ₃ PbI ₃ /Spiro-OMeTAD/Ag		17.4	-0.98	73.7	12.59	
ITO/Au@TiO ₂ -TiAc ₂ -stabilized TiO ₂ /CH ₃ NH ₃ PbI _{3-x} Cl _x /Spiro-OMeTAD/Au	N ₂ atmosphere	22.27	-1.009	74.67	16.78	Ref. 21
ITO/TiAc ₂ -stabilized TiO ₂ /CH ₃ NH ₃ PbI _{3-x} Cl _x /Spiro-OMeTAD/Au		20.78	-1.005	74.26	15.51	
ITO/NiO/3 nm-thick Au film/CH ₃ NH ₃ PbI ₃ /PC ₇₁ BM/Ag	N ₂ -filled	15.9	-0.75	48.6	5.1	Ref. 22
ITO/NiO/CH ₃ NH ₃ PbI ₃ /PC ₇₁ BM/Ag	glove box	10.0	-0.87	36.6	2.6	
ITO/TiO _x -Au NPs-TiO _x /CH ₃ NH ₃ PbI _{3-x} Cl _x /Spiro-OMeTAD/Ag	Glovebox	19.9	-1.08	76	16.2	Ref. 38
ITO/TiO _x /CH ₃ NH ₃ PbI _{3-x} Cl _x /Spiro-OMeTAD/Ag		18.3	-1.00	72	13.2	

“A” indicates that the operating conditions of device are not mentioned in the literature.

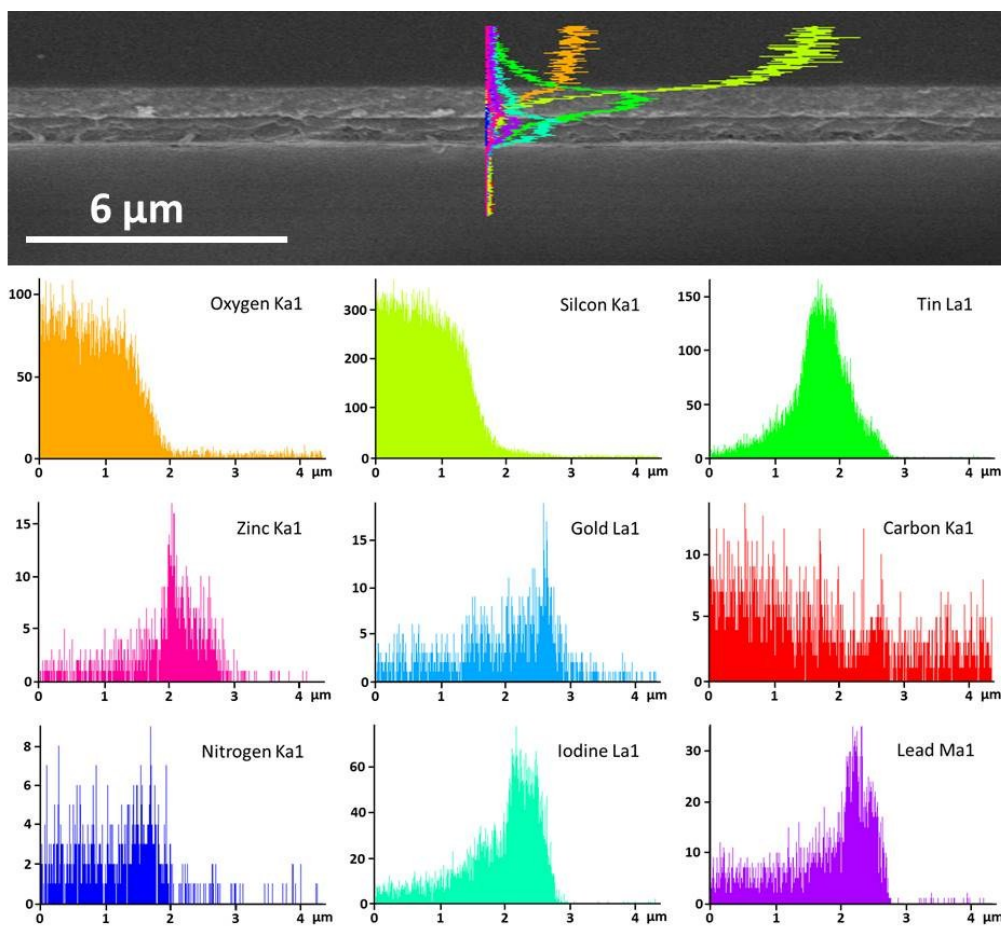


Fig. S1 Cross-sectional SEM image of a complete device based on the structure of glass/FTO/ZnO/Au NRs/MAPbI₃/Spiro-OMeTAD/Au and corresponding EDS line scan of element of O, Si, Sn, Zn, Au, C, N, I and Pb.

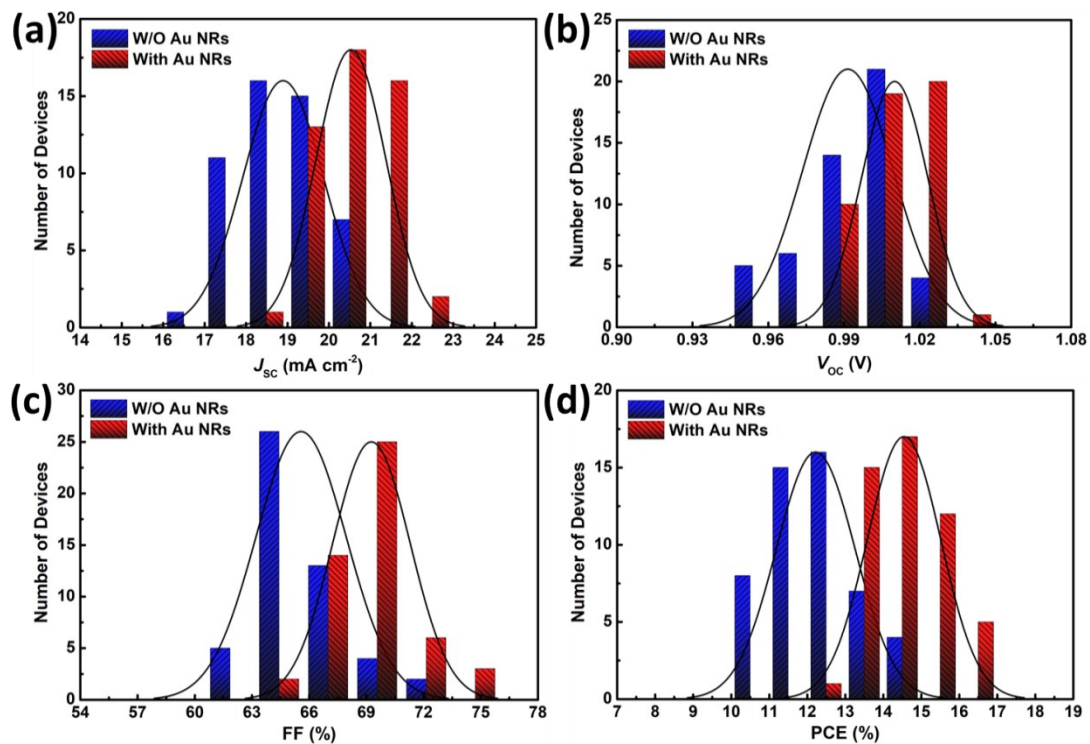


Fig. S2 Statistic distribution histograms of 50 PSC devices with and without Au NRs: (a) J_{sc} , (b) V_{oc} , (c) FF and (d) PCE. The Gaussian fit is provided as a guide to eyes.

$$\text{Hysteresis index} = \frac{J_{\text{RS}}(0.8V_{\text{OC}}) - J_{\text{FS}}(0.8V_{\text{OC}})}{J_{\text{RS}}(0.8V_{\text{OC}})} \quad (1)$$

Equation (1): $J_{\text{RS}}(0.8V_{\text{OC}})$ and $J_{\text{FS}}(0.8V_{\text{OC}})$ represent photocurrent density at 80 % of V_{oc} for the reverse scan (RS) and forward scan (FS), respectively.

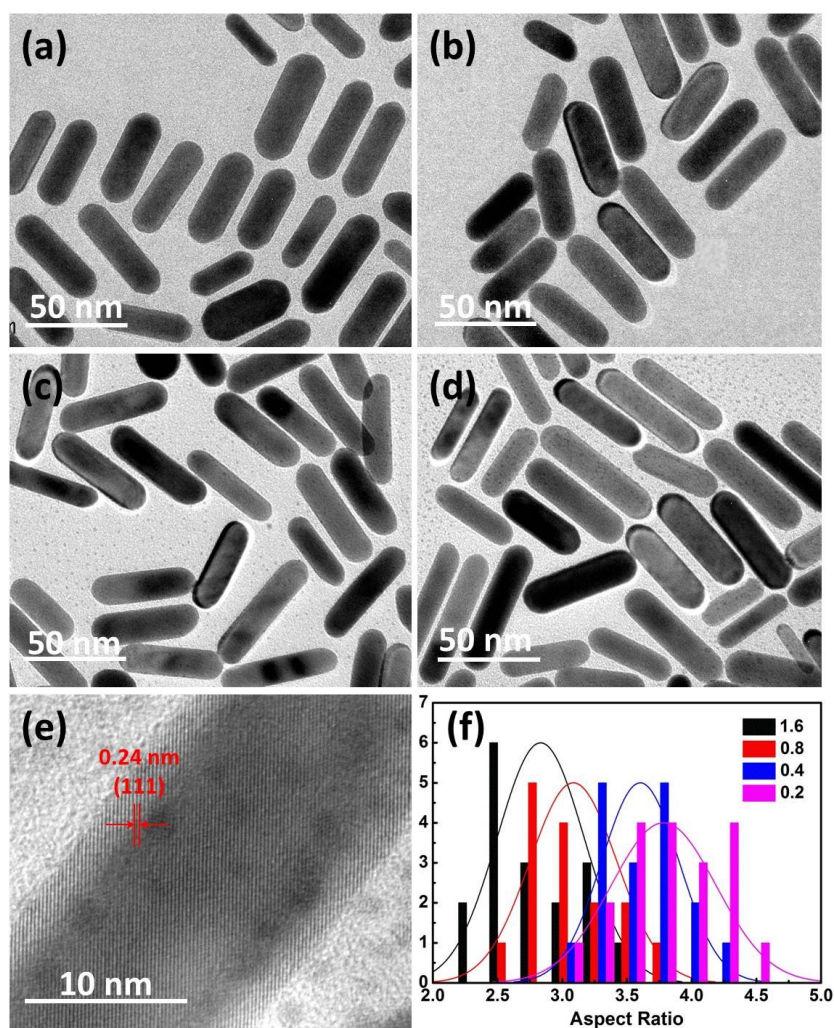


Fig. S3 TEM images of Au NRs obtained from (a) 1.6 mL, (b) 0.8 mL, (c) 0.4 mL and (d) 0.2 mL HCl additives. (e) HRTEM image taken from a single Au NRs. (f) The distribution of aspect ratios of Au NRs measured from Fig. (a) to (d).

Table S2 Average aspect ratio as well as their associated standard deviations of Au NRs obtained by regulating the addition volume of hydrochloric acid.

Data Set	a	b	c	d
Volume of Hydrochloric Acid	1.6	0.8	0.4	0.2
Aspect Ratio	2.83±0.34	3.09±0.34	3.60±0.30	3.80±0.40

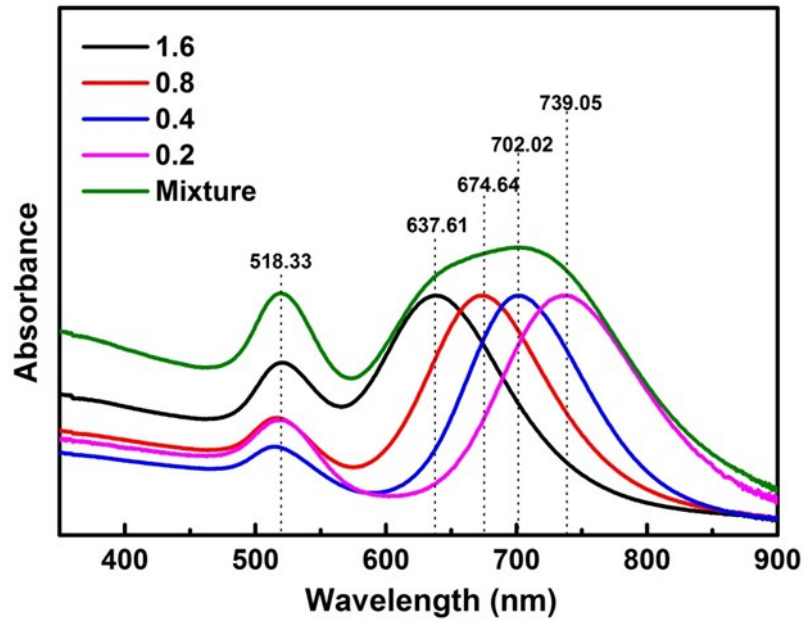


Fig. S4 UV-vis absorption spectra of Au NRs with different aspect ratios and Au NRs mixture.

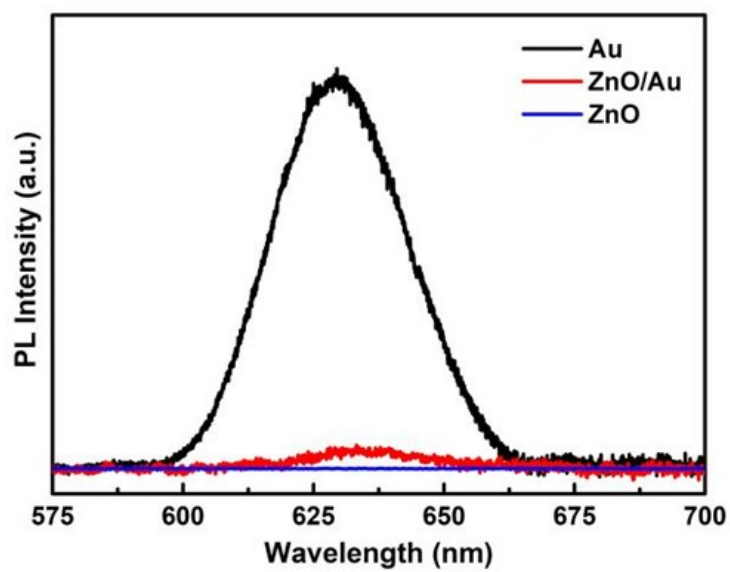


Fig. S5 PL spectra of Au NRs coated on glass and glass/ZnO film as well as pure ZnO film excited by 532 nm laser.

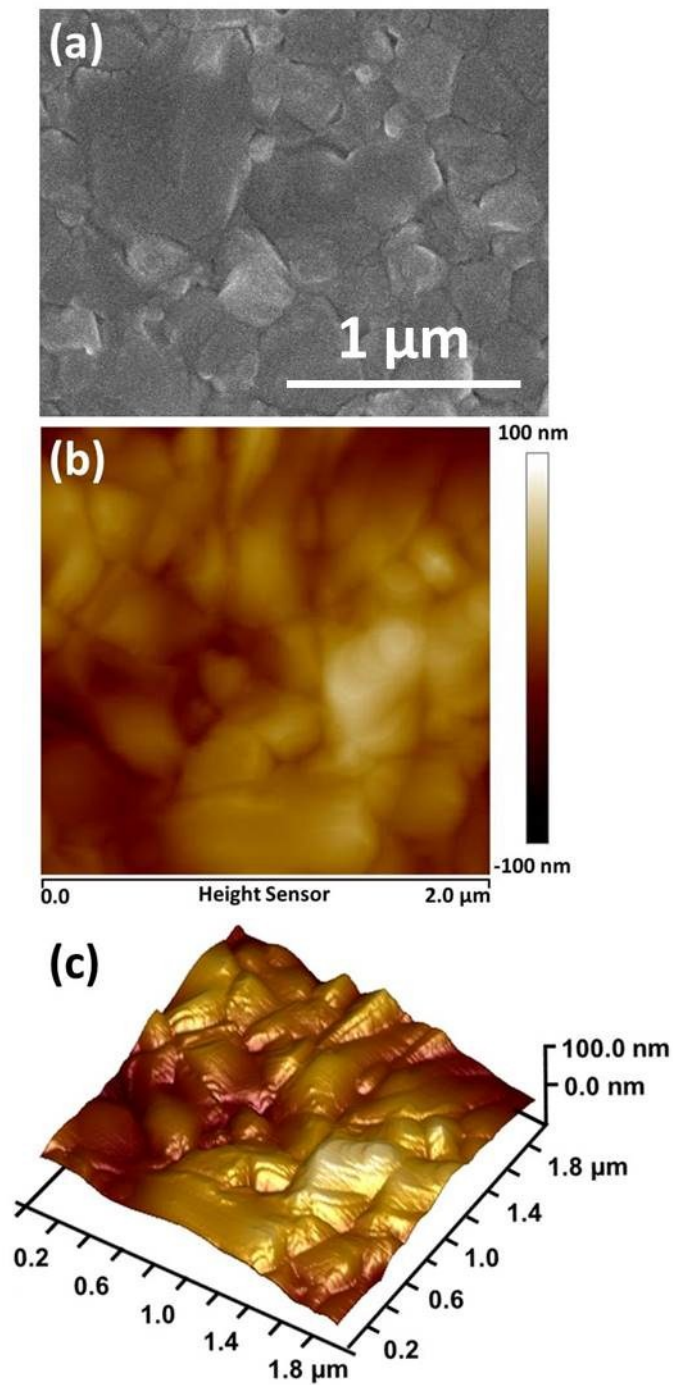


Fig. S6 Top view SEM image (a), AFM height image (b) and corresponding 3D AFM height image (c) of MAPbI_3 coated on the DMF processed ZnO film.

Table S3 Assignments of XRD peaks in Fig. 5a.

2θ (°)	Index	Composite
12.65	001	PbI ₂
13.95	002	MAPbI ₃
14.08	110	MAPbI ₃
19.97	112	MAPbI ₃
23.47	211	MAPbI ₃
24.46	202	MAPbI ₃
26.46	221	MAPbI ₃
28.13	004	MAPbI ₃
28.46	220	MAPbI ₃
31.61	222	MAPbI ₃
31.89	310	MAPbI ₃
33.65	102	PbI ₂
34.96	204	MAPbI ₃
37.70	321	MAPbI ₃
40.48	224	MAPbI ₃
43.14	314	MAPbI ₃

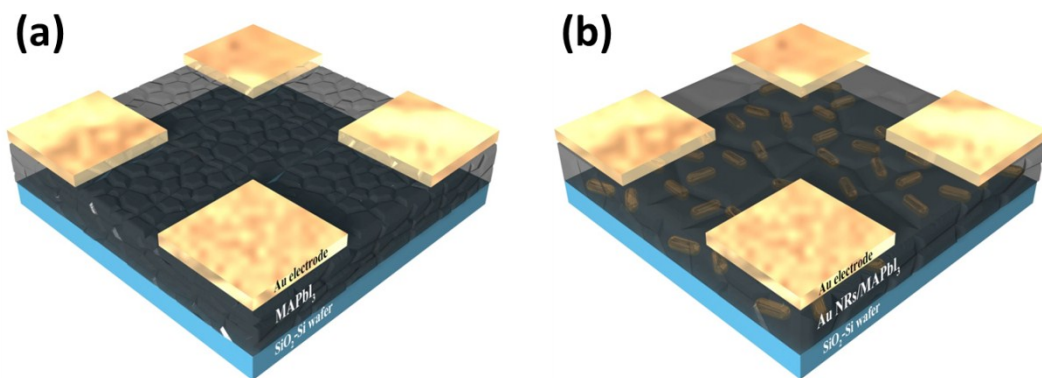


Fig. S7 Structures of devices used to Hall effect measurements. (a) SiO_2 -Si wafer/ MAPbI_3 / Au electrode. (b) SiO_2 -Si wafer/ $\text{Au NRs}/\text{MAPbI}_3$ / Au electrode.

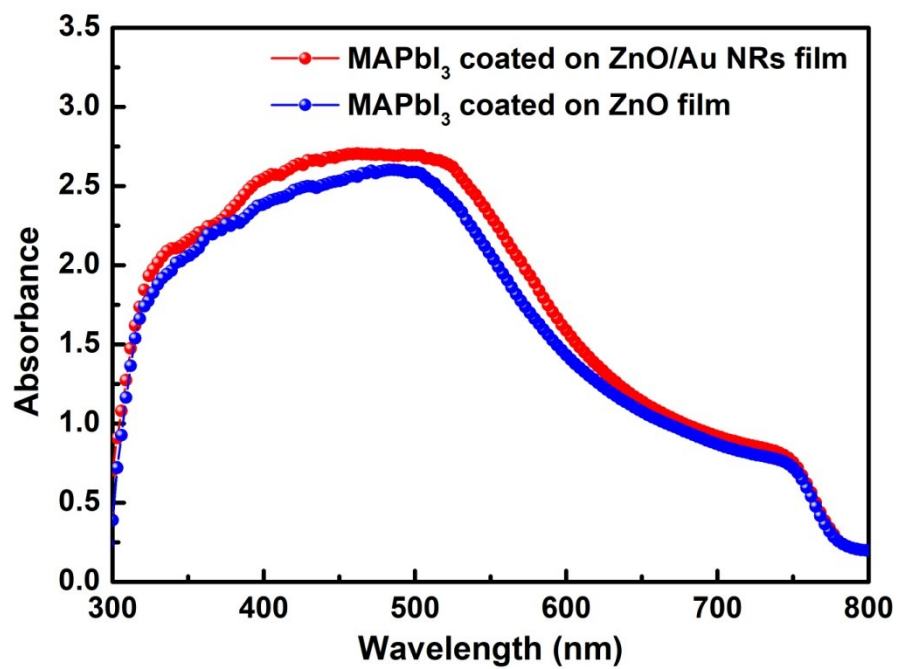


Fig. S8 UV-vis absorption spectra of MAPbI₃ coated on the ZnO and ZnO/Au NRs film.

Table S4 ZView2 fitting parameters obtained from the EIS data of the champion devices with and without Au NRs.

Type	R_S (Ω)	R_{CT} (Ω)	C (F)
Control	13.82	62.15	2.1077 E ⁻⁸
With Au NRs	13.62	33.41	2.4237 E ⁻⁸

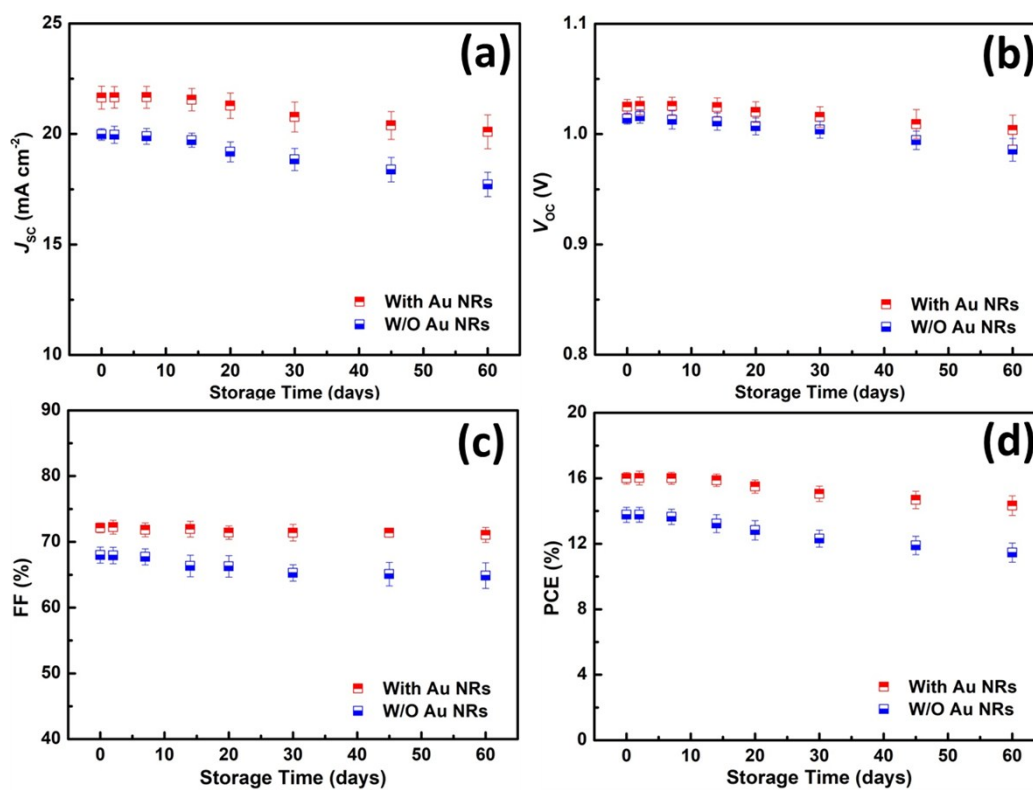


Fig. S9 Changing of (a) J_{sc} , (b) V_{oc} , (c) FF and (d) PCE of ten Au NRs-ZnO-based PSCs and ZnO-based PSCs with the extension of storage period. The devices were stored in an ambient condition with about 40% relative humidity at 25 °C. Error bars represent the standard deviations.

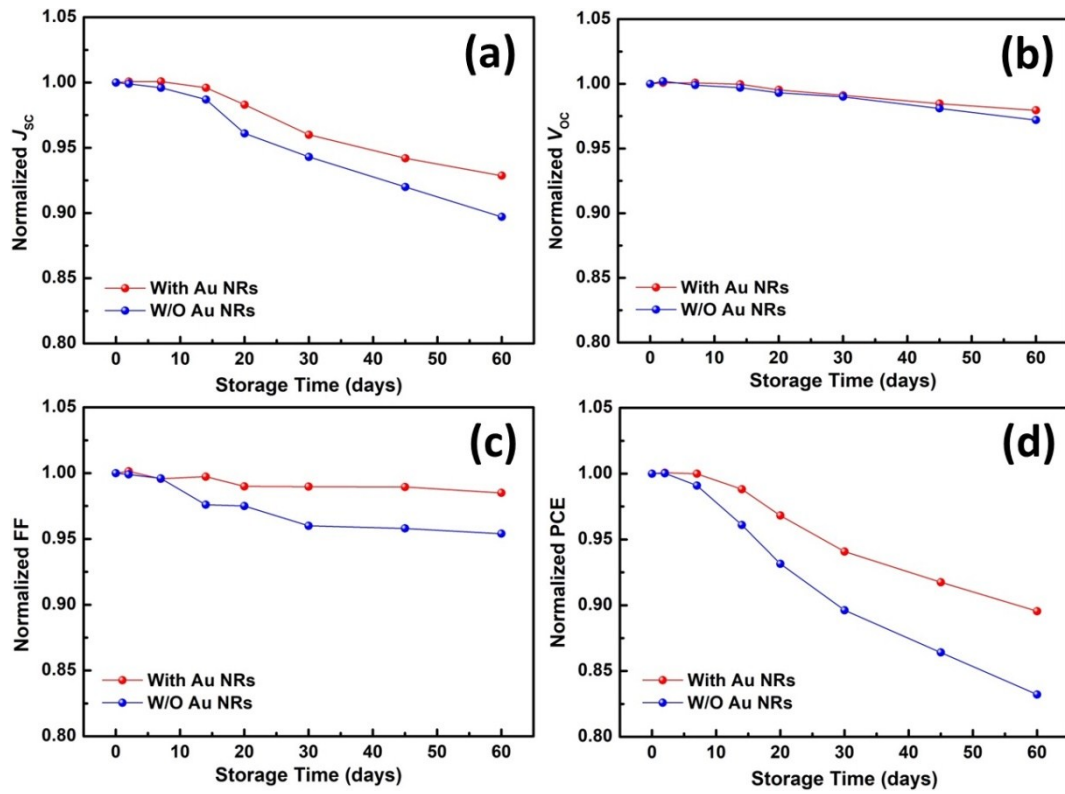


Fig. S10 Changing of normalized (a) J_{sc} , (b) V_{oc} , (c) FF and (d) PCE of ten Au NRs-ZnO-based PSCs and ZnO-based PSCs with the extension of storage period, where the relative humidity and temperature of storage environment are about 40 % and 25 °C, respectively.

Table S5 Performance parameters and normalized performance parameters of ten Au NRs-ZnO-based PSCs with the extension of storage period.

Storage Time (days)	J_{SC} (mA cm ⁻²)/ Normalized J_{SC}	V_{OC} (V)/ Normalized V_{OC}	FF (%)/ Normalized FF	PCE (%)/ Normalized PCE
0	21.64±0.52 / 1.0000	1.0247±0.0067 / 1.0000	72.13±0.75 / 1.0000	16.002±0.356 / 1.0000
2	21.66±0.49 / 1.0009	1.0255±0.0080 / 1.0008	72.23±1.05 / 1.0014	16.014±0.418 / 1.0007
7	21.66±0.50 / 1.0008	1.0255±0.0079 / 1.0008	71.82±1.05 / 0.9957	16.001±0.370 / 0.9999
14	21.55±0.51 / 0.9960	1.0244±0.0084 / 0.9997	71.93±1.20 / 0.9973	15.879±0.378 / 0.9882
20	21.28±0.57 / 0.9830	1.0199±0.0093 / 0.9953	71.40±1.03 / 0.9899	15.493±0.404 / 0.9682
30	20.77±0.68 / 0.9600	1.0156±0.0093 / 0.9911	71.39±1.27 / 0.9897	15.055±0.472 / 0.9408
45	20.39±0.63 / 0.9420	1.0090±0.0132 / 0.9847	71.37±0.66 / 0.9895	14.682±0.531 / 0.9175
60	20.10±0.77 / 0.9286	1.0037±0.0136 / 0.9795	71.05±1.14 / 0.9850	14.329±0.599 / 0.8955

Table S6 Performance parameters and normalized performance parameters of ten ZnO-based PSCs with the extension of storage period.

Storage Time (days)	J_{SC} (mA cm ⁻²)/ Normalized J_{SC}	V_{OC} (V)/ Normalized V_{OC}	FF (%)/ Normalized FF	PCE (%)/ Normalized PCE
0	19.98±0.26 / 1.0000	1.0140±0.0050 / 1.0000	67.98±1.22 / 1.0000	13.770±0.460 / 1.0000
2	19.96±0.38 / 0.9991	1.0160±0.0060 / 1.0020	67.92±1.24 / 0.9991	13.774±0.456 / 1.0003
7	19.90±0.36 / 0.9958	1.0129±0.0082 / 0.9989	67.71±1.23 / 0.9960	13.646±0.466 / 0.9910
14	19.72±0.32 / 0.9870	1.0113±0.0078 / 0.9973	66.34±1.64 / 0.9759	13.232±0.552 / 0.9610
20	19.19±0.45 / 0.9606	1.0070±0.0077 / 0.9931	66.28±1.64 / 0.9750	12.827±0.587 / 0.9315
30	18.85±0.50 / 0.9434	1.0040±0.0077 / 0.9901	65.28±1.23 / 0.9603	12.312±0.519 / 0.8962
45	18.38±0.56 / 0.9202	0.9944±0.0083 / 0.9807	65.09±1.79 / 0.9575	11.899±0.557 / 0.8641
60	17.72±0.55 / 0.8968	0.9857±0.0102 / 0.9721	64.87±1.95 / 0.9543	11.459±0.582 / 0.8322

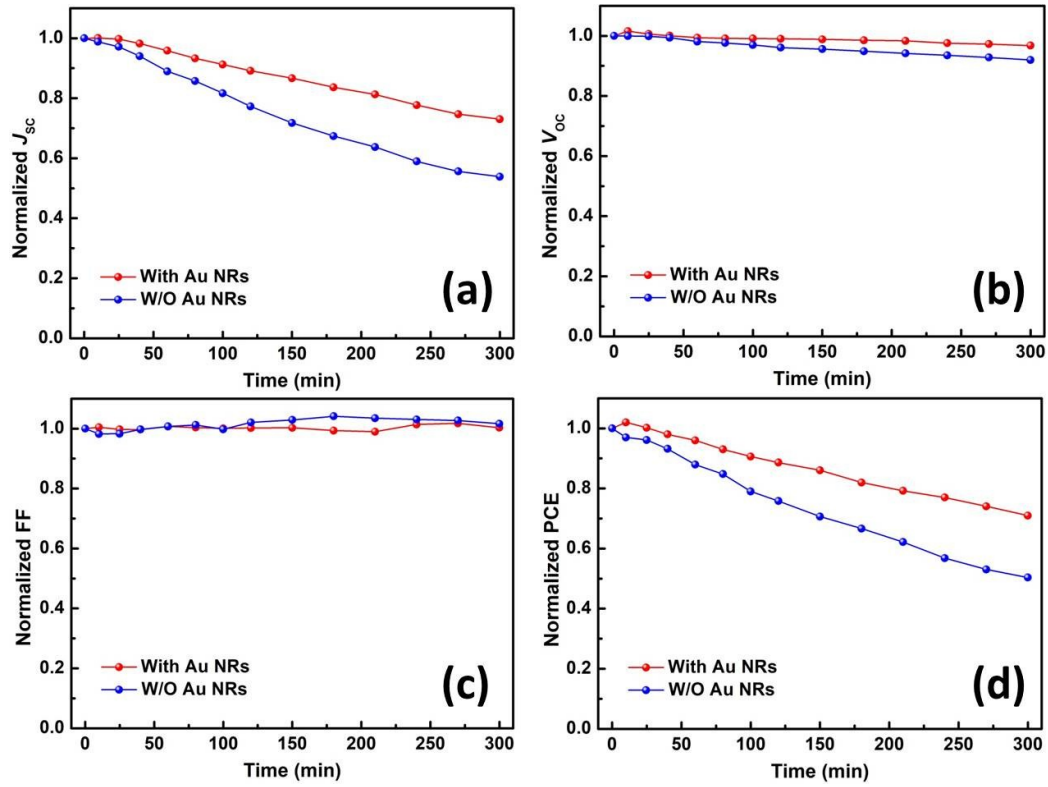


Fig. S11 Changing of normalized (a) J_{sc} , (b) V_{oc} , (c) FF and (d) PCE of ten Au NRs-ZnO-based PSCs and ZnO-based PSCs as a function of illumination time, where the relative humidity and temperature of illumination environment are about 50 % and 25 °C, respectively.

Table S7 Performance parameters and normalized performance parameters of ten Au NRs-ZnO-based PSCs with the extension of illumination time.

Illumination Time (min)	J_{SC} (mA cm ⁻²)/ Normalized J_{SC}	V_{OC} (V)/ Normalized V_{OC}	FF (%)/ Normalized FF	PCE (%)/ Normalized PCE
0	21.89±0.42 / 1.0000	1.0259±0.0062 / 1.0000	71.33±0.75 / 1.0000	15.99±0.25 / 1.0000
10	21.90±0.39 / 1.0005	1.0409±0.0049 / 1.0155	71.65±0.69 / 1.0044	16.31±0.21 / 1.0200
25	21.83±0.35 / 0.9973	1.0321±0.0051 / 1.0060	71.15±0.81 / 0.9975	16.02±0.29 / 1.0019
40	21.50±0.46 / 0.9822	1.0265±0.0053 / 1.0006	71.11±0.79 / 0.9969	15.67±0.31 / 0.9800
60	20.98±0.48 / 0.9584	1.0198±0.0057 / 0.9940	71.84±0.59 / 1.0071	15.35±0.28 / 0.9600
80	20.42±0.51 / 0.9328	1.0173±0.0055 / 0.9916	71.59±0.88 / 1.0036	14.87±0.35 / 0.9300
100	19.97±0.45 / 0.9123	1.0169±0.0064 / 0.9912	71.38±0.89 / 1.0007	14.49±0.29 / 0.9062
120	19.51±0.49 / 0.8913	1.0158±0.0059 / 0.9902	71.49±0.91 / 1.0022	14.17±0.29 / 0.8862
150	18.97±0.50 / 0.8666	1.0142±0.0046 / 0.9886	71.53±0.83 / 1.0028	13.76±0.27 / 0.8605
180	18.31±0.47 / 0.8365	1.0113±0.0048 / 0.9855	70.85±0.90 / 0.9933	13.11±0.31 / 0.8199
210	17.79±0.39 / 0.8127	1.0091±0.0047 / 0.9835	70.60±0.73 / 0.9898	12.67±0.33 / 0.7924
240	17.01±0.43 / 0.7771	1.0013±0.0051 / 0.9757	72.31±0.94 / 1.0137	12.31±0.24 / 0.7699
270	16.35±0.54 / 0.7469	0.9980±0.0062 / 0.9728	72.58±0.78 / 1.0175	11.84±0.35 / 0.7405
300	15.98±0.49 / 0.7300	0.9933±0.0053 / 0.9679	71.54±0.90 / 1.0029	11.35±0.34 / 0.7098

Table S8 Performance parameters and normalized performance parameters of ten ZnO-based PSCs with the extension of illumination time.

Illumination Time (min)	J_{SC} (mA cm ⁻²)/ Normalized J_{SC}	V_{OC} (V)/ Normalized V_{OC}	FF (%)/ Normalized FF	PCE (%)/ Normalized PCE
0	19.20±0.53 / 1.0000	1.0021±0.0057 / 1.0000	67.32±0.92 / 1.0000	12.95±0.37 / 1.0000
10	18.97±0.59 / 0.9880	1.0017±0.0051 / 0.9996	66.12±0.87 / 0.9822	12.56±0.42 / 0.9699
25	18.65±0.48 / 0.9714	1.0007±0.0049 / 0.9986	66.16±0.94 / 0.9828	12.45±0.31 / 0.9614
40	18.05±0.57 / 0.9401	0.9961±0.0059 / 0.9939	67.15±0.75 / 0.9975	12.07±0.43 / 0.9320
60	17.08±0.61 / 0.8896	0.9832±0.0063 / 0.9811	67.82±0.63 / 1.0074	11.39±0.37 / 0.8795
80	16.46±0.45 / 0.8573	0.9785±0.0061 / 0.9764	68.16±0.91 / 1.0124	10.98±0.41 / 0.8479
100	15.68±0.49 / 0.8167	0.9718±0.0049 / 0.9698	67.15±0.69 / 0.9976	10.23±0.45 / 0.7900
120	14.84±0.39 / 0.7729	0.9631±0.0063 / 0.9611	68.70±0.72 / 1.0205	9.82±0.39 / 0.7583
150	13.78±0.49 / 0.7177	0.9581±0.0058 / 0.9561	69.28±0.59 / 1.0290	9.15±0.43 / 0.7066
180	12.94±0.54 / 0.6740	0.9509±0.0069 / 0.9489	70.11±0.90 / 1.0414	8.63±0.42 / 0.6664
210	12.24±0.60 / 0.6375	0.9439±0.056 / 0.9419	69.67±0.78 / 1.0349	8.05±0.46 / 0.6216
240	11.32±0.43 / 0.5896	0.9373±0.0054 / 0.9353	69.38±0.68 / 1.0306	7.36±0.42 / 0.5683
270	10.68±0.37 / 0.5563	0.9302±0.0063 / 0.9282	69.15±0.73 / 1.0272	6.87±0.45 / 0.5305
300	10.34±0.52 / 0.5385	0.9217±0.0062 / 0.9198	68.41±0.89 / 1.0162	6.52±0.35 / 0.5035

References

- 1 Y. Guo, L. Kang, M. Zhu, Y. Zhang, X. Li and P. Xu, *Chem. Eng. J.*, 2018, **336**, 732-740.
- 2 X. Ye, C. Zheng, J. Chen, Y. Gao and C. B. Murray, *Nano Lett.*, 2013, **13**, 765-771.